Chemical Engineering Research and Design 201 (2024) 433–445

Contents lists available at ScienceDirect

Chemical Engineering Research and Design

journal homepage: www.elsevier.com/locate/cherd

Investigation of different configurations of alumina packed bed reactor for coke free conversion of benzene

Waqar Ahmad *, Leteng Lin, Michael Strand

Department of Built Environment and Energy Technology, Linnaeus University, 35195 Växjö, Sweden

ARTICLE INFO

Keywords:
Benzene conversion
Polymerization reactions
Coke generation
Packed bed
Reforming media

ABSTRACT

Conversion of producer gas tar without coke generation is a great challenge. This study investigates conversion of tar model benzene using different configurations of highly non-porous ɣ-Al_2O_3 packed bed reactor at 1000–1100 ^{0}C. The configurations comprised of different positions (relative to top (P_1), center (P_2) and bottom (P_3) of reactor furnace), heights (5, 13 and 25 cm) and particles sizes (0.5, 3 and 5 mm) of alumina packed bed. Steam and CO_2 were used as reforming media for tested benzene concentrations (0.4–1.8 vol%). The results showed benzene conversions of 48–91% with negligible steady thin coke generation using a packed bed (height: 25 cm, particles size: 3 mm) at P_1. Whereas, relative high benzene conversions of 63–93 and 68–95% at P_2 and P_3 respectively with unsteady thick coke generation at benzene concentrations greater than 0.4 vol% increased differential upstream pressures (DUPs) of beds. Similar unsteady coke generation at benzene concentrations greater than 0.8 vol% and temperature of 1100 ^{0}C was observed with packed beds of heights of 5 and 13 cm, and particles size of 0.5 mm at P_1. Generation of unsteady coke with condensed structure as evidenced by its characterization was attributable to increased benzene polymerization and reduced bed surface gasification reactions due to improperly installed packed bed. Developed kinetic model predicted well the generated coke. As conclusion, properly installed alumina packed bed pertaining to tar concentration and other experimental conditions may inhibit coke generation during tar conversion.

1. Introduction

Biomass valorization through thermochemical conversion presents a promising alternative source of renewable energy with respect to continuously depleting fossil fuels (Shen and Fu, 2018; Shen and Yoshikawa, 2013). The most common thermochemical conversion approach of gasification converts the biomass to combustible producer gas (CPG) (Larsson et al., 2021). CPG can be used either for combined heat and power generation or for synthesis of value-added chemicals (Lin and Strand, 2013, 2014). CPG from gasifier downstream requires upgrading to meet the specifications at end use. It involves the removal of inorganic aerosol particulates, sulfur impurities and particularly the tar content. Tar is a condensable part of CPG and majorly composed of complex mixture of aromatic hydrocarbons (Gómez Cápiro et al., 2021; Ahmad et al., 2022; Gao et al., 2022). Tar condensation in downstream assembly causes operational and environmental problems such as fouling and equipment breakdown, and polluting the underground water respectively (Morgalla et al., 2018a, 2018b; Wang et al., 2022; Madadkhani et al., 2021a). The usual high tar content (5–100 g/Nm^3) of CPG required to be reduced to 20 mg/Nm^3 for useful applications (Gómez-Barea and Leckner, 2010). Tar conversion to either combustible gases (e.g., CO, CH_4, H_2) or lighter hydrocarbons with lower dew points is energy efficient instead of its complete removal from CPG (Wang et al., 2022; Zhang et al., 2023). Therefore, catalytic reforming and thermal cracking techniques convert the tar to synthesis gas and are more attractive than mechanical methods removing it entirely (Ahmad et al., 2022; Zhang et al., 2021; Li et al., 2022). However, undesired formation of polycyclic aromatic hydrocarbons (PAHs) due to tar polymerization may occur under thermal severity (high temperature and long residence time). Further possible polymerization of PAHs may lead to coke generation (Houben et al., 2002; Zhai et al., 2015). Catalytic reforming is extensively used technique due to efficient tar conversion at low temperatures. However, the deposition of generated coke over the active sites of catalysts such as organometallic/transition metal (e.g., Cu, Fe, Ni, Mn) based compounds and minerals (e.g., iron ores, calcined rocks, dolomite, zeolite) causes their deactivation (Wang et al., 2020; Madadkhani et al., 2021b; Cheng et al., 2020; Cao et al., 2018). Liu et al. (2017) observed appreciable coke deposition on acidic sites of metals

* Corresponding author.
E-mail address: waqar.ahmad@lnu.se (W. Ahmad).

https://doi.org/10.1016/j.cherd.2023.11.063
Received 23 August 2023; Received in revised form 7 November 2023; Accepted 29 November 2023
Available online 2 December 2023

(Co, Mo and Ni) loaded HZSM-5 catalysts during significant reduction of pyrolysis tar yield from 21.4% to 11.9%. Wang et al (Wang et al., 2011). noticed relatively low and high coke deposition on Ni-Fe/Al_2O_3 and Ni/Al_2O_3 catalysts respectively during complete conversion of cedar wood pyrolysis tar at temperatures above 873 K. Similar coke deposition over the catalysts used for tar conversion have been greatly reported in literature reviews (Shen et al., 2013; Han and Kim, 2008; Dayton, 2002; Ashok et al., 2020).

Conventional thermal cracking technique for significant tar conversion also experiences PAHs/coke generation influenced by various parameters (e.g., temperature, concentration of reforming media, residence time). Gilbert et al. (2009) thermally reduced the woody pyrolysis tar yield from 37.6 wt% to 15.3 wt% at 800 ^{0}C. However, the reduced tar was greatly comprised of PAHs. Zhang et al. (2006) observed coke generation during sawdust pyrolysis at 900–1100 ^{0}C. Whereas, no appreciable coke generation probably due to increased gasification with complete tar elimination at high temperature of 1200 ^{0}C was observed. Wu et al. (2011) observed increasing conversion of O-containing and substituted 1-ring aromatics to PAHs at increasing temperatures during thermal cracking of pyrolysis tar. Brandt and Henriksen (Brandt and Henriksen, 1998) noticed soot and PAHs in outlet gas and condensate respectively during thermal cracking of pyrolysis gas and updraft producer gas tar at 800–1000 ^{0}C. High tar conversion of 98–99% was achieved. Zhai et al. (2015) achieved complete thermal conversion of dry husk pyrolysis tar to non-condensable gases and char/coke at 1300 ^{0}C. Houben et al. (2002) thermally reduced the producer gas tar content of 2 g/Nm^3 to 0.2 g/Nm^3 at residence time of 12 s and temperature of 1150 ^{0}C. However, a larger part of tar and small hydrocarbons were converted to soot through polymerization reactions.

Application of different bed materials for tar conversion in high-temperature reactors without coke generation was investigated. Hosokai et al. (2005) investigated the thermal cracking and steam reforming of biomass pyrolysis tar in silica sand and Al_2O_3 fixed bed reactors. Significant yields of coke deposits were observed in both reforming modes with both tested beds. Shimizu et al. (2007) observed the coke over mesoporous Al_2O_3 during conversion of pyrolysis tar. Zeng et al. (2018) also observed the coke over Al_2O_3 placed in reforming reactor of two-stage fluidization apparatus during thermal conversion of coal pyrolysis tar. de Caprariis et al. (2019) noticed deactivation of bed materials (activated carbon, aluminum oxide, olive residue char and pumice stone) due to coke deposition during conversion of biomass pyrolysis tar.

Above-mentioned literature revealed that both catalytic reforming and thermal cracking techniques converted the tar significantly but with appreciable generation of coke due to tar polymerization. However, research efforts were made to investigate the various aspects of coke generation during tar conversion. Chen et al. (2022) investigated the effect of steam and CO_2 as reforming media on filamentous coke deposition during conversion of non-oxygenates tar in presence of Ni/bio-char catalyst. Relative low coke deposition in case of steam atmosphere than in CO_2 atmosphere lead high tar conversion. Similar findings of low coke deposition over biochar catalyst was reported in a coke generation investigation during conversion of corn straw pyrolysis tar in presence of steam (Sun et al., 2021a). Sun et al. (2022) investigated biochar alkali and alkaline earth metals (AAEMs) influence on conversion of biomass pyrolysis tar and generated coke characteristics. The observed O-containing structured coke over Ca and K loaded biochar lead relative significant high tar conversion of 94.9% than 27.8% achieved with aliphatic structured coke over acid washed biochar. Li et al. (2021a) investigated coke deposition during microwave catalytic cracking and thermal catalytic cracking of toluene and phenol in presence of Ni-Ce/SiC catalyst. Relative suppressed coke generation with microwave catalytic cracking than significant coke generation with thermal catalytic cracking was observed. Sun et al. (2021b) investigated mechanism of coke generation during biochar catalyzed conversion of corn straw pyrolysis tar. Increased tar aromatization and methane cracking on biochar surface were suggested as possible pathways for coke generation. In another investigation, increased mutual interactions of volatile radical fragments or with char during coal pyrolysis were suggested as possible reasons of coke generation (Li et al., 2021b). Zhang et al. (2010) investigated tar conversion and coke generation during pyrolysis, steam gasification and partial oxidation of woody waste. The results indicated that coke generation could be influenced by competition between secondary decomposition of hydrocarbon species and gasification of in situ produced coke. Another study about toluene conversion over activated carbon revealed competition reactions responsible for determining the proportions for toluene conversion to benzene and coke (Korus et al., 2017). Related to catalysts development, Tian et al. (2022a) reduced the coke yield from 48% to 6% during toluene reforming by developing core-shell structure and cobalt doping in Ni/ZrO_2 catalyst. In another study, appropriate thickness of SiO_2 shell layer in core-shell catalysts with mesoporous and microporous silica-coated nickel nanoparticles achieved reduced coke generation during toluene conversion (Tian et al., 2022b). Since, most of the investigations related to coke generation as shown above were greatly about factors influencing the coke generation, coke evaluation mechanisms and characterization of generated coke with a limited focus on avoiding the coke generation. Therefore, configuring a reactor assembly avoiding the conversion of tar to coke and rather directing that to combustible gases was urgently needed. Recently, authors developed a novel highly non-porous ɣ-Al_2O_3 packed bed reactor to investigate the conversion of tar model benzene. High benzene conversions of 52–84% with negligible steady coke deposits on bed particles attributing to combined effect of packed bed surface and high temperatures were achieved (Ahmad et al., 2023). However, this study is a next stage research investigating the effects of different configurations of developed ɣ-Al_2O_3 packed bed reactor on benzene conversion at 1000–1100 ^{0}C. These configurations are mainly comprised of modified packed beds with their different positions, heights and particles sizes. The reactor configurations generating coke during benzene conversion at different experimental conditions of temperatures and concentrations of benzene and reforming media (steam and CO_2) are identified. Selection of benzene as a tar model instead of producer/pyrolysis gas is due to fundamental nature of presented tar conversion investigation, for which a simple primary tar component is more convenient to track the conversion behavior/path. That could be either syngas or PAHs/coke formation through polymerization reactions. In addition, benzene appeared to be the most scarcely convertible/cracked tar component during producer/pyrolysis gas tar conversion studies (Houben et al., 2002; Zhang et al., 2010). A kinetic model is developed to estimate the coke generated under different experimental conditions. Moreover, the generated coke samples are characterized to understand the effect of experimental conditions and reactor configuration on conversion behavior of benzene and coke formation itself.

2. Materials and methodology

2.1. Materials

Benzene (purity level: 99.7%, Merck, Kenilworth, NJ, USA) was used as a tar model. N_2 and CO_2 with purity levels of 99% from Air Liquide AB, Sweden were used as carrier and reforming gases respectively. The ɣ-Al_2O_3 particles (T-162; Almatis GmbH, Ludwigshafen, Germany) within different average size ranges (e.g., 0.5, 3 and 5 mm) and mean pore diameter of 0.71 μm were used as a packed bed. The ɣ-Al_2O_3 particles with average sizes of 0.5 and 3 mm were irregular while particles with average size of 5 mm were spherical in shape.

2.2. Experimental setup

The experimental setup mainly involves three sections; gas feeding, packed bed reactor and gas analysis as shown in Fig. 1. Gas feeding section dealt with controlled supply of steam and benzene carrier N_2 and

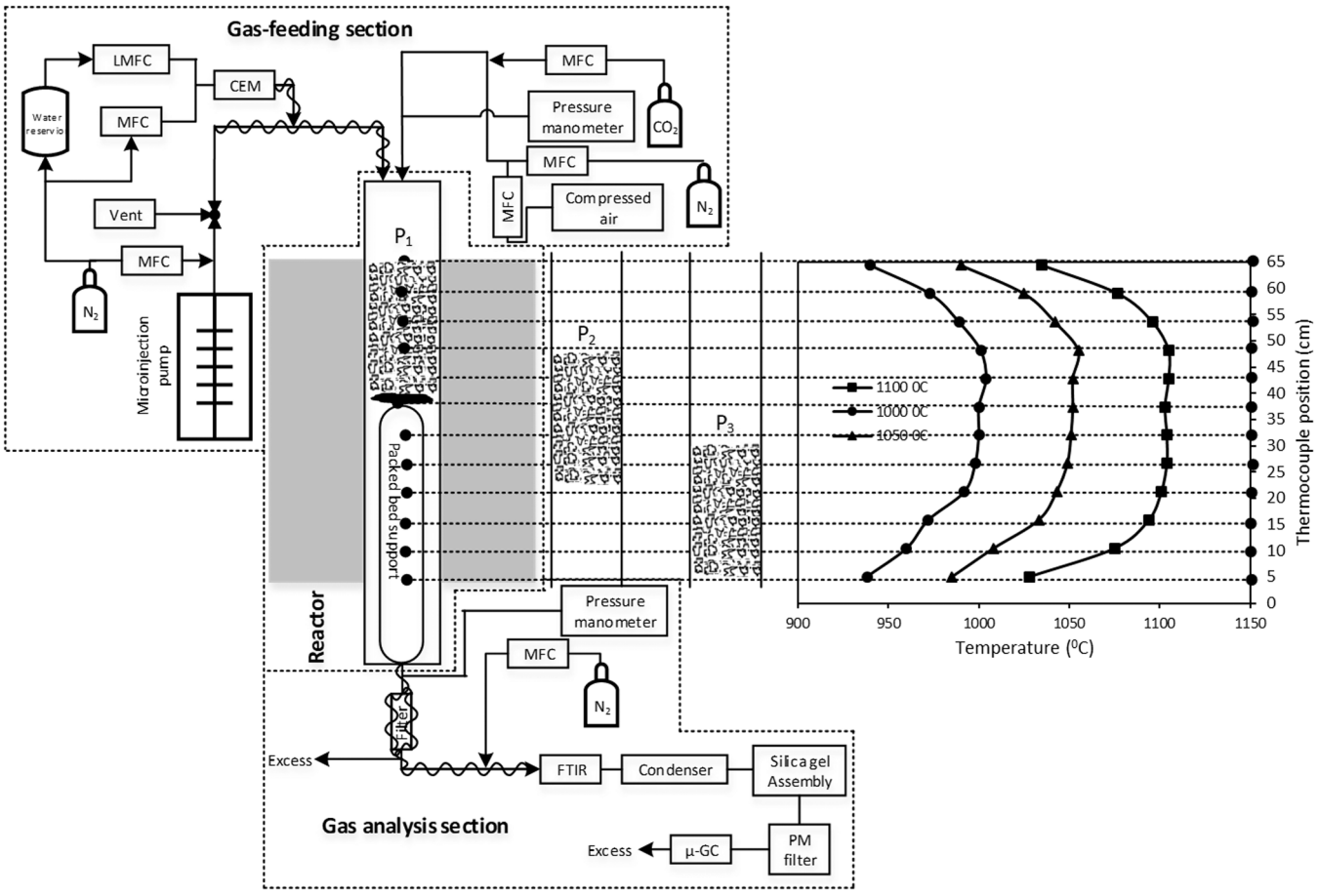

Fig. 1. Experimental setup with different packed bed positions and reactor temperature profile.

CO_2 using mass flow controllers (MFCs) (Bronkhorst High-Tech, Ruurlo, Netherlands). Benzene was supplied using a microinjection pump (CMA/100; Stockholm, Sweden) through a concentration stabilizer. Steam was generated using controlled evaporation and mixing (CEM) unit and its concentration was regulated by adjusting the water flow using liquid mass flow controller (LMFC) (Bronkhorst High-Tech). Gas feeding section was kept heated at 130 ^{0}C to avoid steam condensation.

The reactor used in this study is a ceramic vertical tubular reactor (Pythagoras tube; Morgan Advanced Materials, Windsor, England) with inside diameter of 27 mm. The ɣ-Al_2O_3 packed beds of various heights (5, 13 and 25 cm) and particle sizes (0.5, 3 and 5 mm) at different positions relative to reactor furnace dimension (P_1: top of furnace, P_2: center of furnace and P_3: bottom of furnace) were installed inside the reactor. The reactor assembly was heated at desired temperature using an electrically heated tube furnace (Entech Energiteknik AB, Ängelholm, Sweden). The temperature of packed bed was measured using K-type thermocouple.

Gas analysis section dealt with inspection of outlet gases (e.g., CO, CO_2, CH_4, steam and benzene) at reactor downstream. A high temperature (HT) thimble filter was installed at reactor downstream to capture any generated soot/coke particle and ensure contaminant free clean gas entering the gas analysis section. The concentrations of outlet gases were measured using a Fourier transform infrared (FTIR) gas spectrometer (type DX-4000; Gasmet Technologies Oy, Helsinki, Finland). To adjust the concentrations of outlet gases within the measuring range of the FTIR, the entering gas was diluted with N_2. The concentrations of gases were corrected afterwards. The gas exiting the FTIR was led to cold trap and silica gel assembly before directing to micro gas chromatograph (model CP-4900; Varian Inc., Palo Alto, CA, USA) for measuring the H_2 concentration. The upstream pressures of both packed bed and HT filter were continuously monitored using pressure meters (Elcanic, Type PTM 100).

2.3. Experimental procedure

Experiments were initiated by heating the packed bed reactor at 300 ^{0}C under N_2 supply. N_2 supply was replaced with flow of benzene, reforming media and N_2 carrier gas shortly after the stable reactor temperature reached. Assuming measured benzene concentration at 300 ^{0}C as a baseline, the reactor temperature was raised to desired temperature of benzene conversion. After attaining the stable reactor temperature and concentrations of outlet gases, the experimental run was continued for a collective 70–90% of benzene inlet flow rate unless any coke generation initiated. In case of generation of coke and its continuous accumulation over packed bed could clog the packed bed causing a continuous rise in its differential upstream pressure (DUP). On other side, generated coke may possibly penetrate through the packed bed and accumulate inside the HT filter causing increases in both HT filter and packed bed DUPs. The packed bed/HT filter DUP is defined as the difference in its upstream pressures at a certain time during the experimental run and baseline for benzene conversion.

Experimental runs generating the coke were continued up to packed bed/HT filter DUP of 10–30 kPa, after that the experiment was stopped by diverting the benzene flow and stopping the supply of reforming media. Moreover, the visual inspection of both packed bed reactor and HT filter was performed after cooling it down to ambient temperature under N_2 supply. Before commencing the repetition or next experiment, the reactor was cleaned by gasifying/combusting any retained hydrocarbon/carbon deposit particles using a mixture of steam and excess air at high temperature. Each experiment presented in this study is repeated

two times to affirm the repeatability and determine the standard deviation represented as an error bar.

The coke deposits were not quantified as that was not the focus of this study. The measured concentrations of reactor outlet gases have not been presented as well, since those were not also relevant to aimed investigation. The detailed experimental conditions are given in Table 1. Since, this study focuses on both benzene conversion and any coke generation with different packed bed configurations at different experimental conditions, therefore, all the tabulated experiments were not performed. For instance, coke generation during conversion of low benzene concentration would eliminate the testing of conversion of next higher benzene concentration at similar experimental conditions.

The reactor outlet gas flow rate was calculated using the N_2 balance:

$$Q_{in}.y_{N_2,in} = Q_{out}.y_{N_2,out} \quad (1)$$

where Q_{in} and Q_{out} are the reactor inlet and outlet gas flow rates respectively. Likewise, $y_{N_2,in}$ and $.y_{N_2,out}$ represent the concentrations (vol%) of N_2 in reactor inlet and outlet gas respectively. $y_{N_2,out}$ was computed through subtraction the summation of measured concentrations of other outlet gas components (e.g., CO, CO_2, CH_4, H_2, C_6H_6, steam).

The benzene conversion was calculated using the expression:

$$X = \left[\frac{y_{C_6H_6,in} - y_{C_6H_6,out}}{y_{C_6H_6,in}}\right] * 100 \quad (2)$$

where X represents the benzene conversion.

Similarly, the carbon percentage error ($C_{\%E}$), another indicator of coke generation, can be determined using the expression:

$$C_{\%E} = \overline{\left[\frac{C_{in} - C_{out}}{C_{in}}\right]} * 100 \quad (3)$$

where C_{in} (g/min) $= \sum_0^{t_E} \frac{Q_{in}.M_C.\left\{y_{CO_2,in}+y_{C_6H_6,in}\right\}.\Delta t}{V_M}$ and C_{out} (g/min) $= \sum_0^{t_E} \frac{Q_{out}.M_C.\left\{y_{CO,out}+y_{CO_2,out}+y_{CH_4,out}+y_{C_6H_6,out}\right\}.\Delta t}{V_M}$; V_M (L/mol) is the molar volume of an ideal gas at normal temperature and pressure (i.e., 20 °C and 1 bar), M_C (g/mol) is the molar mass of carbon, t_E is total time of the experiment, and Δt (min) is the time interval between two data points.

2.3.1. Coke modeling

A simple kinetic model was developed to estimate the coke generated at different temperatures and benzene concentrations. Plug flow reactor conditions are assumed to compute the kinetically limited gas phase reactions. Reactions considered in model development with their kinetic parameters and reaction rates are listed in Table 2. Steam and dry reforming, and cracking reactions are the possible reactions occurring during benzene conversion. Dry reforming of generated coke (C (s)) instead of benzene is considered due to its observed negligible and significant effects on benzene conversion and quantified generated coke respectively during combined steam and CO_2 reforming of benzene. A detailed pathway about conversion of benzene to coke with intermediate conversion to higher aromatics and PAHs is avoided due to unavailability of detailed kinetic data and computation complexity.

The reactor is assumed to be divided into many small cylindrical cells. The computations in each cell were performed by solving the set of partial differential equations given as Eq. (4) using 4th order Runge-Kutta method. The inputs in a cell are temperature simulated by experimentally determined temperature profile and the concentrations of components leaving the former cell as shown in Fig. 2.

$$\frac{\partial y_i}{\partial V} = \sum r_i / Q \quad (4)$$

Table 2
Reactions used in model development (rate units: $kmolm^{-3}s^{-1}$, concentration units: $kmolm^{-3}$).

	Reactions	Rate expressions	Ref.
1	$C_6H_6 + 5H_2O \rightarrow 5CO + 6H_2 + CH_4$	$r_1 = k_1[C_6H_6]$ $k_1 = 4.4 \times 10^8 \exp\left(\frac{-2.2 \times 10^5}{RT}\right)$	(Virk et al., 1974)
2	$C_6H_6 + 2H_2O \rightarrow 1.5C(s) + 2CO + 2.5CH_4$	$r_2 = k_3[C_6H_6]^{1.3}[H_2O]^{0.2}$ $k_2 = 3.39 \times 10^{16} \exp\left(\frac{-4.43 \times 10^5}{RT}\right)$	(Jess and Erdgas, 1995)
3	$C_6H_6 \rightarrow 6C(s) + 3H_2$	$r_3 = k_5[C_6H_6]$ $k_3 = 6.6 \times 10^7 \exp\left(\frac{-1.85 \times 10^5}{RT}\right)$	(Virk et al., 1974)
4	$C(s) + H_2O \rightarrow CO + H_2$	$r_4 = k_6[H_2O][C(s)]$ $k_4 = 3.6 \times 10^{12} \exp\left(\frac{-3.1 \times 10^5}{RT}\right)$	(Jess, 1996)
5	$C(s) + CO_2 \rightarrow 2CO$	$r_5 = k_5 P_{CO_2}^{0.31}$ $k_5 = 1.12 \times 10^{18} \exp\left(\frac{-2.45 \times 10^8}{RT}\right)$	(Watanabe et al., 2002)

P_{CO_2} is partial pressure of CO_2, Pa.

Table 1
Experimental conditions.

Type of investigation	Effect of packed bed position	Effect of packed bed height, cm	Effect of packed bed particles size, mm	Effect of concentration of reforming media, vol%		Effect of gas flow rate, slpm
				Steam reforming	*CO_2 reforming*	*Gas flow rate*
Benzene concentration (vol %)	0.4, 0.8, 1.5, 1.8	0.4, 0.8, 1.5, 1.8	0.4, 1.5, 1.8	0.4	0.4	0.8
Steam concentration (vol %)	24	24	24	11.5, 16.5, 24	24	24
CO_2 concentration (vol%)	17	17	17	17	0, 6, 12, 17	17
Gas flow rate (slpm)	0.85	0.85	0.85	0.85	0.85	0.85, 1.25, 2
Steam to carbon molar ratio, S/C[a]	1.8, 1.6, 1.4, 1.3	1.8, 1.6, 1.4, 1.3	1.8, 1.4, 1.3	0.8, 0.95, 1.8	17.8, 4.5, 2.7, 1.8	1.6
Reactor Temperature (^{0}C)	1000, 1050, 1100	1000, 1050, 1100	1000, 1050, 1100	1000, 1050, 1100	1000, 1050, 1100	1000, 1050, 1100
Packed bed position	P_1, P_2, P_3	P_1	P_1	P_3	P_3	P_1
Packed bed height, cm	25	5, 13, 25	25	25	25	25
Packed bed particles average size (mm)	3	3	0.5, 3, 5	3	3	3
Packed bed gas residence time (s)	1.86[b], 1.79[c], 1.72[d]	0.37, 0.35, 0.34; 0.96, 0.93, 0.89; 1.86, 1.79, 1.72	1.86, 1.79, 1.72	1.86, 1.79, 1.72	1.86, 1.79, 1.72	1.86, 1.79, 1.72; 1.27, 1.22, 1.18; 0.79, 0.76, 0.73

a: carbon both from benzene and CO_2 flow; b, c, d: first, second and third place values at 1000, 1050 and 1100 ^{0}C respectively for a specific packed bed height or gas flow rate.

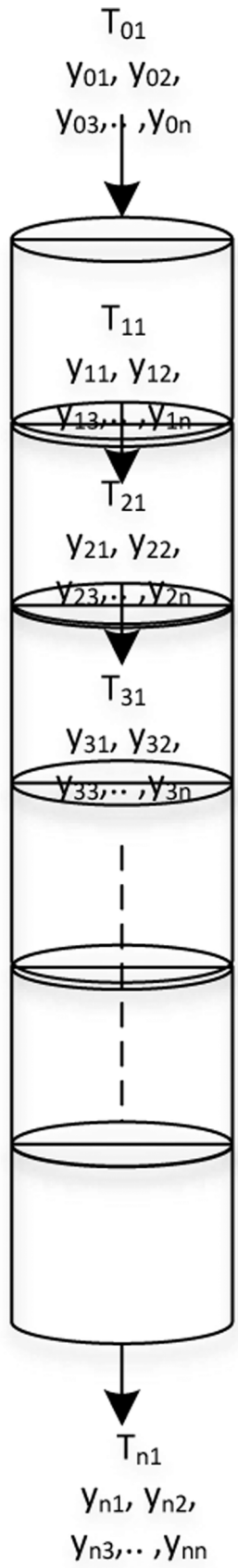

Fig. 2. Computation scheme of developed kinetic model.

where V (m^3) is reactor volume and r ($kmolm^{-3}s^{-1}$) is rate of reaction.

2.3.2. Coke characterization

The coke generated during benzene conversion was collected and characterized using thermogravimetric analyzer (TGA, Q500 from TA instrument supplied by Waters LLC) and FTIR spectrometer (Bruker, Vertex 80 v). In TGA analysis, 5 mg of coke was placed in alumina crucible and temperature was increased from ambient temperature to 900 ^{0}C at a rate of 10 ^{0}C/min under air supply of 45 mL/min. The sample temperature was maintained at 900 ^{0}C for 30 min. Differential thermogravimetric (DTG) curves were computed to investigate the thermo-oxidative behaviors of cokes. FTIR spectrometry of coke (1 wt% in KBr) was performed in the wavenumber range (4000–400 cm^{-1}) with a resolution of 4 cm^{-1}.

3. Results and discussion

3.1. Effect of packed bed position

Conversions of tested benzene concentrations achieved at considered packed bed (height: 25 cm, particles size: 3 mm) positions and reactor temperatures are shown in Fig. 3(a)-(c). Decrease in benzene conversion with an increase in tested benzene concentration at a particular packed bed position and temperature is obvious. For instance, benzene conversions decrease from 61 to 48, 69 to 63 and 76 to 68% at P_1, P_2 and P_3 respectively with increase in benzene concentration from 0.4 to 1.8 vol % at 1000 ^{0}C. Likewise, benzene conversions in range of 79–66, 82–71 and 90–75% at P_1, P_2 and P_3 respectively at 1050 ^{0}C, and benzene conversions in range of 91–83, 93–87 and 95–91% at P_1, P_2 and P_3 respectively at 1100 ^{0}C were achieved. However, thermal influence with increased benzene conversions at increased temperatures was also obvious. Conversions of all the tested benzene concentrations at P_1 were without the rises in DUPs of packed bed and HT filter. Whereas, conversions of benzene concentrations greater than 0.4 vol% at P_2 and P_3 showed rise in DUPs of packed beds that could be due to coke generation. The accumulation of generated coke over the packed beds and its no gasification could lead blockage of the packed beds causing continuous increase in their DUPs as shown in Fig. 3(d)-(f). Higher $C_{\%E}$ for conversions of different benzene concentrations at P_2 and P_3 than at P_1 are in line and obvious from Fig. 3(a)-(c). Moreover, the visual inspection of packed beds and reactor walls in case of P_2 and P_3 revealed significant unsteady thick layers of coke compared to negligible steady thin layers in case of P_1. Similar findings of negligible steady thin coke layers on bed particles were observed in earlier investigation (Ahmad et al., 2023). Conversions of benzene concentrations generating coke have been shown as red filled in symbols in Fig. 3(a)-(c). The findings are in accordance with earlier reported mechanism of tar conversion of its conversion first into coke through secondary polymerization reactions and then the subsequent conversion of coke into gases (H_2, CO, CO_2) through gasification reactions (Hosokai et al., 2008). Whereas, coke generated at P_2 and P_3 than at P_1 appear more resistant to gasification. That could be because of more condensed structures of coke generated at P_2 and P_3 than at P_1 due to relatively increased homogeneous benzene polymerization reactions, neglecting the effect of reactor walls, at greater residence times. However, gasification-resistant characteristic of coke could lead an unsteady state due to relatively high rate of coke generation than gasification at P_2 and P_3 than at P_1. Therefore, coke generated at P_2 and P_3, and P_1 may be described as unsteady and steady coke respectively.

Comparing the benzene conversions achieved at considered packed bed positions under similar experimental conditions showed the trend $P_3 > P_2 > P_1$. That could also because of the influence of residence time for benzene homogeneous reforming/polymerization on benzene conversion; greater the benzene homogeneous reforming/polymerization higher would be the benzene conversion. Thermal homogenous

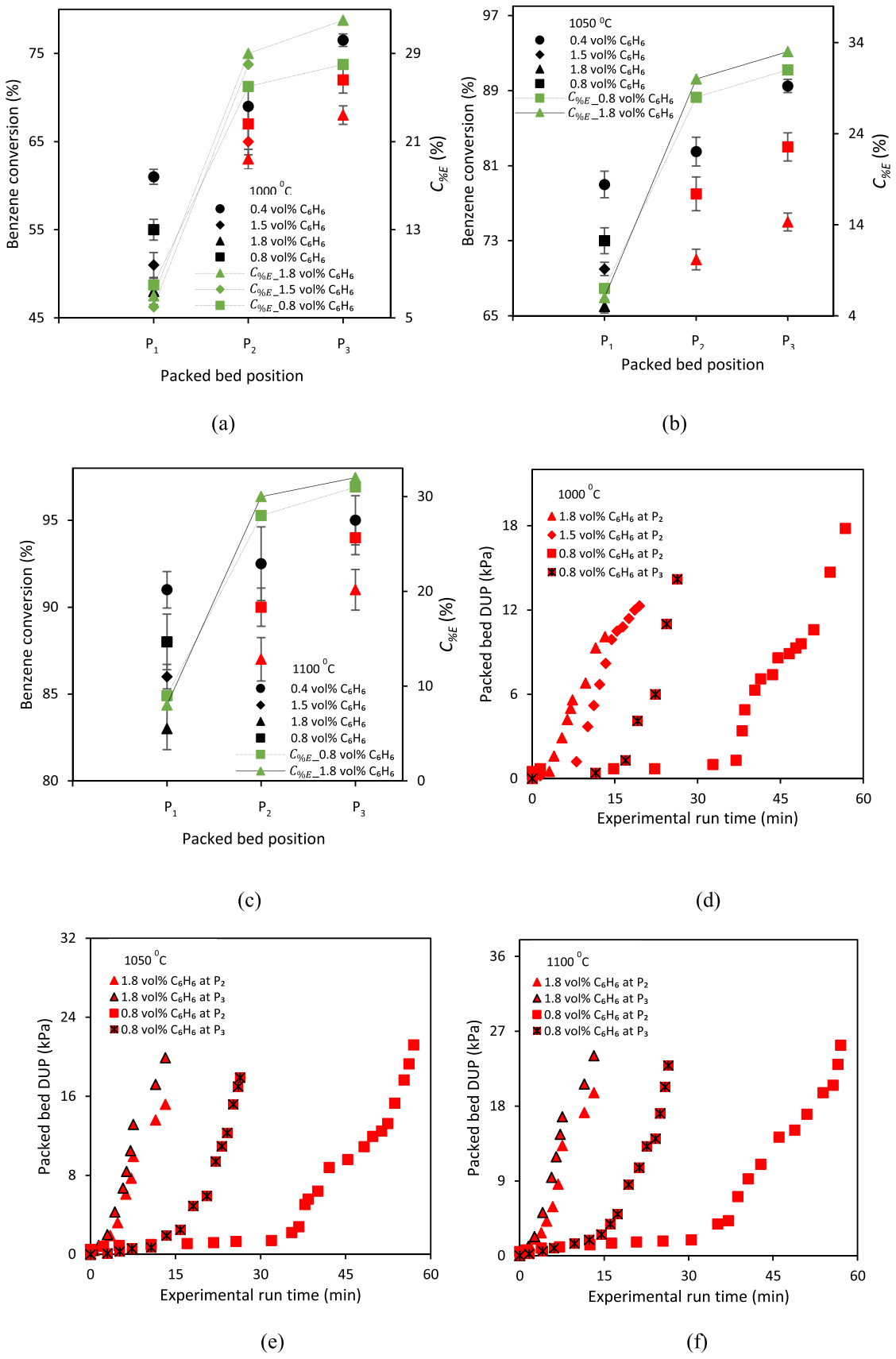

Fig. 3. Conversions of tested benzene concentrations and corresponding $C_{\%E}$ at different packed bed positions and temperatures in (a-c) with red filled in symbols showing generation of coke, and corresponding rise in packed bed DUP during coke generation in (d-f).

reforming was identified as the main route of tar conversion (Gilbert et al., 2009).

Careful data analysis also identified the factors influencing the coke generation during benzene conversion. Fig. 3(d)-(f) show the influences of residence time for benzene homogeneous reforming/polymerization, benzene concentration and reactor temperature on coke generation. Earlier coke generation during conversions of benzene concentrations of 0.8 and 1.8 vol% with greater time homogeneous reforming at P_3 than shorter time homogeneous reforming at P_2 are visible in Fig. 3(e)-(f). Earlier coke generation during conversion of high benzene concentration of 1.8 vol% than low benzene concentration of 0.8 vol% as visible in Fig. 3(d)-(f) shows an increasing trend of coke generation with increasing benzene concentration. Quicker coke generation during conversions of benzene concentrations of 0.8 and 1.8 vol% at high temperature than at low temperature at a particular packed bed position as visible from figures reveals a significant influence of temperature on coke generation. Several studies have reported similar influences of parameters like residence time, temperature, heating rate, and composition on tar reforming/polymerization reactions responsible for coke formation (Serio et al., 1987; Xu and Tomita, 1989).

3.1.1. *Effect of packed bed height*

Fig. 4(a)-(c) shows the conversions of tested benzene concentrations achieved with different packed bed (position: P_1, particles size: 3 mm) heights at different reactor temperatures. Nearly similar conversions of a benzene concentration were achieved with considered packed bed heights at a particular reactor temperature. For tested benzene concentration of 1.5 vol% at 1050 ^{0}C, benzene conversions of 72, 71 and 70% with 5, 13 and 25 cm packed beds respectively, were achieved. Benzene conversions of 81, 85 and 82% with 5, 13 and 25 cm packed beds respectively were achieved for benzene concentration of 1.8 vol% at 1100 ^{0}C. That revealed no particular influence of packed bed height on benzene conversion and thus achieved nearly similar conversions of tested benzene concentrations as achieved with packed bed position P_1 in "Effect of packed bed position". However, decreasing and increasing trends of benzene conversion with increasing benzene concentration and temperature respectively are obvious from Fig. 4(a)-(c). Therefore, benzene conversions of approximately 62–51, 82–66 and 92–81% at 1000, 1050 and 1100 ^{0}C respectively were achieved for tested benzene concentrations of 0.4–1.8 vol% with considered packed bed heights.

All the tested benzene concentrations were converted with 25 cm packed bed without a rise in packed bed/HT filter DUP. However, conversions of benzene concentrations of 1.5 and 1.8 vol% both with 13

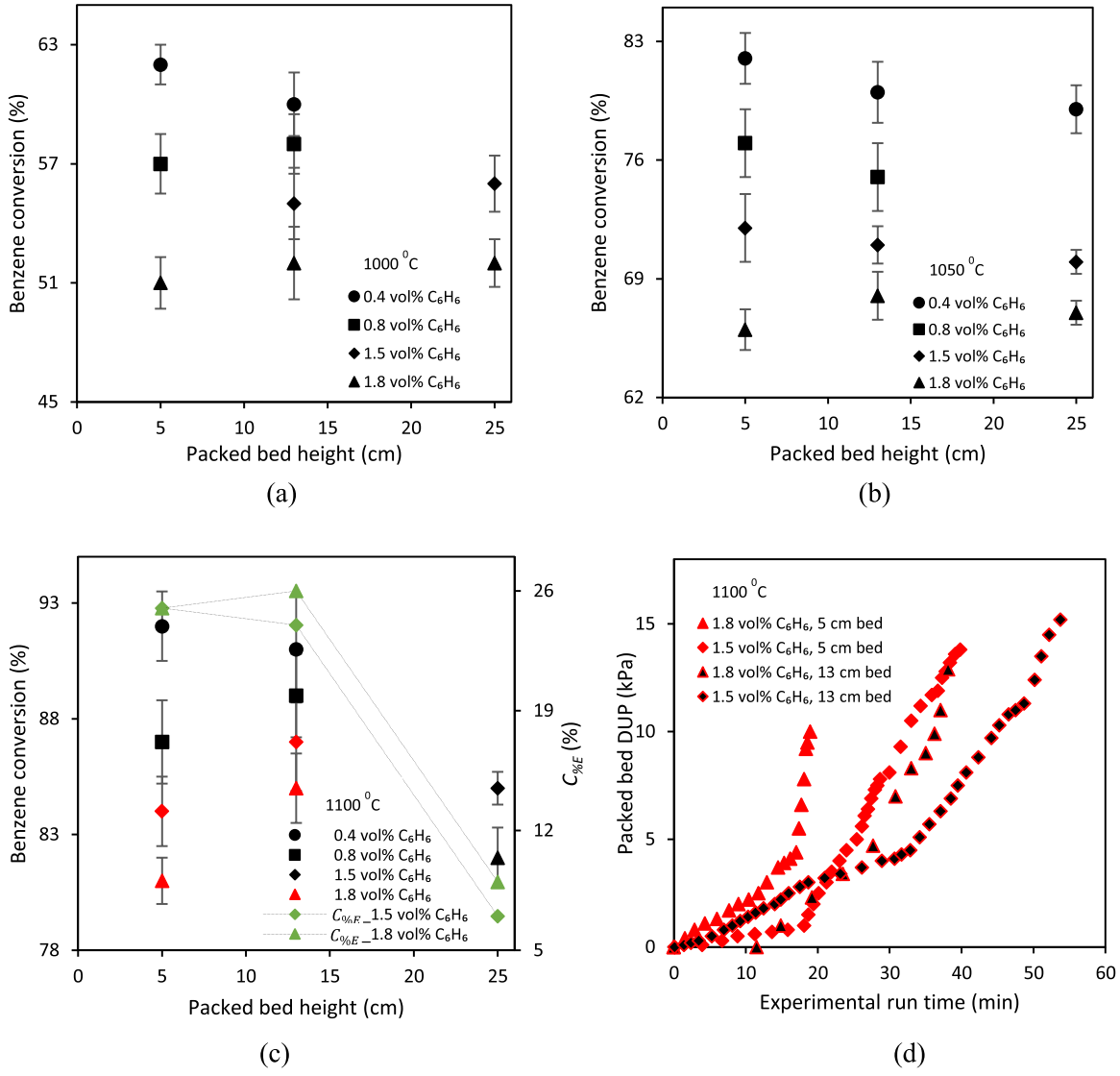

Fig. 4. Conversions of tested benzene concentrations with different packed bed heights at different temperatures in (a-c) with red filled in symbols showing generation of coke, and corresponding rise in packed bed DUP during coke generation in (d).

and 5 cm packed beds at 1100 ^{0}C observed continuous increase in packed beds DUPs. It could be again due to coke generation as observed during conversions of benzene concentrations greater than 0.4 vol% at P_2 and P_3 in "Effect of packed bed position". Corresponding high $C_{\%E}$ with 5 and 13 cm packed beds than with 25 cm packed bed are evident in Fig. 4(d). Moreover, the visual inspection of reactors with 5 and 13 cm packed beds showed the beds blockage with thick coke. Conversions of these benzene concentrations have been shown as red filled in symbols in Fig. 4(c). Packed beds of 5 and 13 cm could exhibit relatively high inlet carbon to packed bed mass ratios than 25 cm packed bed. That could result into decreased gasification of generated coke through reduced surface reactions, which lead increasing coke accumulation over beds particles and ultimately blockage of packed beds. Similar findings of increasing coke generation at increasing biomass fed carbon during conversion of biomass pyrolysis tar in an alumina fixed bed reactor were observed (Hosokai et al., 2005). Influence of benzene concentration on coke generation with earlier coke generation during conversion of benzene concentration of 1.8 vol% than benzene concentration of 1.5 vol% under similar experimental conditions is also visible from Fig. 4(d).

3.1.2. *Effect of packed bed particles size*

Conversions of tested benzene concentrations achieved with packed bed (position: P_1, height: 25 cm) particles of various sizes at different reactor temperatures are shown in Fig. 5(a)-(c). Similar tendency of no particular effect of packed bed height on benzene conversion and achieving nearly similar conversions of a tested benzene concentration with different bed heights at a particular reactor temperature was observed with tested bed particles. Benzene conversions of 54, 51 and 55% with bed particles of 0.5, 3 and 5 mm respectively were achieved for tested benzene concentration of 1.5 vol% at 1000 ^{0}C. Testing benzene concentration of 0.4 vol% achieved benzene conversions of 80, 79 and 82% with 0.5, 3 and 5 mm bed particles respectively at 1050 ^{0}C. However, generally observed decreasing benzene conversions with increasing benzene concentrations are evident from Fig. 5(a)-(c). Therefore, benzene conversions of 62–50, 82–65 and 93–81% at 1000, 1050 and 1100 ^{0}C respectively were achieved for tested benzene concentrations with packed beds of considered particles sizes.

All the tested benzene concentrations were converted without a rise in packed bed/HT filter DUP with 3 and 5 mm bed particles. Whereas, the conversion of benzene concentration of 1.5 vol% at 1100 ^{0}C with 0.5 mm bed particles experienced a continuous increase in packed bed

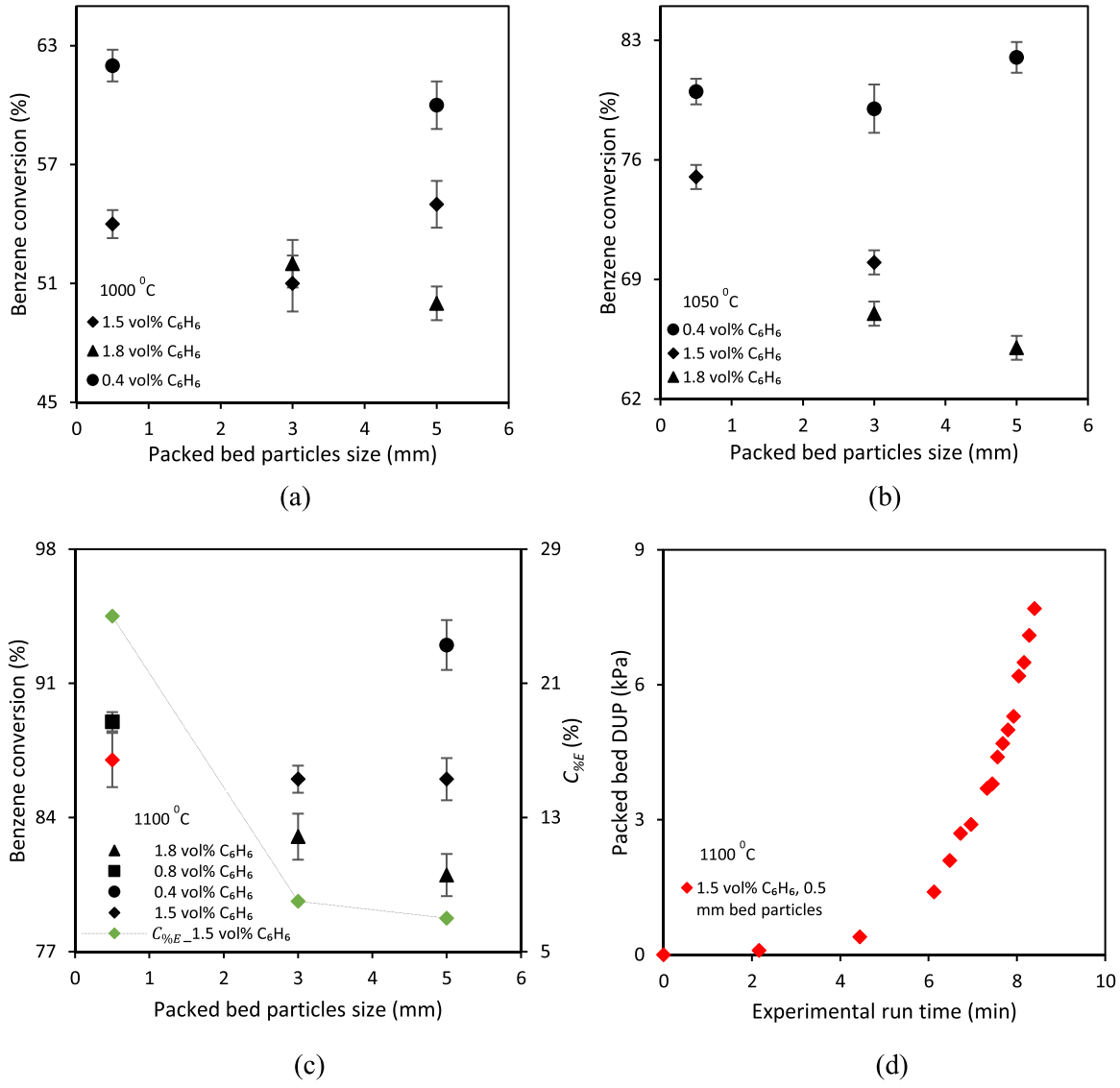

Fig. 5. Conversions of tested benzene concentrations with various packed bed particles sizes at different temperatures in (a-c) with red filled in symbols showing generation of coke, and corresponding rise in packed bed DUP during coke generation in (d).

DUP as shown in Fig. 5(d). Corresponding high $C_{\%E}$ with 0.5 mm bed particles than with 3 and 5 mm bed particles is visible from Fig. 5(c). However, the visual inspection of packed bed reactor indicated loose thick coke over top of the packed bed while rest of the packed bed at downstream was free of any coke particle. That revealed the obstruction of generated coke across the dense closely packed bed and thus could reduce the bed surface reactions responsible for its gasification. This benzene conversion with coke generation has been shown as red filled in symbol in Fig. 5(c).

3.1.3. Effect of concentration of reforming media and gas flow rate

Fig. 6(a)-(d) shows conversions of benzene concentration of 0.4 vol% at different concentrations of reforming media with a packed bed (position: P_3, height: 25 cm, particles size: 3 mm) reactor. Varying the concentration of either reforming medium did not influence the benzene conversion. Nearly similar benzene conversions of 77, 84 and 83% at steam concentrations of 24, 16.5 and 11.5 vol% respectively were achieved at 1000 ^{0}C. Likewise, different tested CO_2 concentrations (0, 6, 12 and 17 vol%) also resulted into approximately similar average benzene conversions of 72, 87 and 92% at 1000, 1050 and 1100 ^{0}C respectively as shown in Fig. 6(b)-(d).

Benzene conversions at reduced steam concentrations of 11.5 and 16.5 vol% in contrast to 24 vol% experienced rises in packed bed DUPs as shown in Fig. 6(e). Higher $C_{\%E}$ at steam concentrations of 11.5 and 16.5 than at 24 vol% were estimated as shown in Fig. 6(a). Moreover, the visual inspection of the packed bed reactors in case of 11.5 and 16.5 vol% steam showed the blockage of packed beds with solid thick coke. These benzene conversions have been shown as red filled in symbols in Fig. 6(a). The coke generation at reduced steam concentrations could be because of steam to carbon (S/C) molar ratios lower than one. That could reduce the gasification/decomposition of generated coke and resulted into its continuous accumulation. However, the rises in packed beds DUPs were established at comparatively longer experimental run times than the ones observed in abovementioned cases. That could be attributed to relatively low rate of coke generation due to tested low benzene concentration of 0.4 vol% in this case than high rates of coke generation due to tested high benzene concentrations of 0.8–1.8 vol% in abovementioned cases. That again revealed the influence of benzene concentration on coke generation during conversion. On other side, reduction in CO_2 concentration even its termination did not cause an increase in packed bed/HT filter DUP and consequently no coke generation.

Fig. 6(f) shows the conversions of benzene concentration of 0.8 vol% achieved at different gas flow rates and temperatures with a packed bed (position: P_1, height: 25 cm, particles size: 3 mm) reactor. Decrease in benzene conversion with an increase in gas flow rate at a particular temperature is evident from figure. It could be attributed to decreased gas residence time with increase in gas flow rate that had significant impact on benzene conversion.

4. Benzene conversion kinetics

The benzene conversion data without the coke generation from this experimental study could be used to establish a general model for tar conversion in used experimental setup. Assuming plug flow conditions and no effect of excess reforming media on benzene conversion, the benzene conversion with a packed bed configuration follows a single first order kinetic equation:

$$\frac{dC_6H_6}{d\tau} = kC_6H_6 \tag{5}$$

τ (kg m^{-3} h) is weight time and is defined as ratio of packed bed mass to gas flow rate. Using weight time instead of gas residence time may account the impact of both packed bed and gas residence time as both have significant influence on benzene conversion. The apparent reaction rate constant, k (m^3 kg^{-1} h^{-1}), the expression of that as given in Eq. (6) could be derived from Eq. (5).

$$k = \frac{-\ln(1-X)}{\tau} \tag{6}$$

This approach of first order kinetic equation to estimate the tar conversion using k has been widely used (Morgalla et al., 2018b; Delgado et al., 1996; Narváez et al., 1997). Rearranging Eq. (6) gives:

$$X = (1 - \exp(-k\tau)) \times 100 \tag{7}$$

Fig. 7 shows the benzene conversions as a function of τ at 1000–1100 ^{0}C. Eq. (7) was fitted to achieved experimental benzene conversions and plots for estimated benzene conversions are shown in Fig. 7. The estimated k has been reported in Table 3. Analyzing the trend of plot at 1000 ^{0}C indicates that 95% benzene conversion can be achieved at τ greater than 6 kg m^{-3} h. Similar with plots at 1050 and 1100 ^{0}C; benzene conversions of 95% at τ values of 3.17 and 2.1 kg m^{-3} h respectively.

5. Coke modeling

Fig. 8 shows the estimated coke in comparison to experimentally determined coke at different experimental conditions of packed bed position, temperature and benzene concentrations. Estimated increasing coke generation at increasing temperature and benzene concentration is in line with experimentally determined coke. A good agreement between estimated and experimental coke is visible although relatively high and low estimated coke. The relatively low estimated coke could be due to kinetically established gasification reactions compared to reduced/hindered gasification reactions as observed with bed heights of 5 and 13 cm, and particles size of 0.5 mm. Whereas, estimated high coke could be because of increased gasification reactions due to bed surfaces at bed position P_2 and P_3 relative to similar established gasification reactions. The other reasons could be the other reactions involving decomposition of benzene and generated coke not included in reactions considered for model development.

6. Coke characterization

6.1. TGA analysis

Due to greatly reported significant effect of temperature on coke formation and its structural characteristics, coke generated during benzene conversion at different temperatures irrespective of packed bed specifications was collected and characterized (Xu and Tomita, 1989; Alexander et al., 1962; Wu et al., 2017). Fig. 9 shows the TG/DTG curves from non-isothermal oxidation of coke generated at 1000, 1050 and 1100 ^{0}C. Slightly lower temperature oxidation of coke generated at 1000 ^{0}C than high temperatures oxidation of coke generated at 1050 and 1100 ^{0}C is visible. The maximum oxidation rate of the coke generated at 1000 ^{0}C occurred at 593 ^{0}C whereas, coke generated at 1050 and 1100 ^{0}C showed its maximum oxidation rate at 600 and 606 ^{0}C respectively. Similar results of increasing temperature of maximum oxidation rate of a coke at its increasing formation temperature have been reported (Ren et al., 2007; Ranjbar, 1995). That was attributed to high condensed structure of coke generated at high temperature than low condensed structure of coke generated at low temperature. The difference in coke structures may contribute to their oxidation kinetics. Assuming no mass transfer limitations due to small coke sample and excess of purge gas outside the sample pan, the non-isothermal coke oxidation can be described by first order Arrhenius equation as given by Eq. (8) (Kök, 2008).

$$\ln[(dW/dt)/W] = \ln A - E/RT \tag{8}$$

where $\ln[(dW/dt)/W] = ln(k')$. dW/dt is rate of mass change, E is activation energy, A is Arrhenius constant and k' is apparent oxidation rate constant.

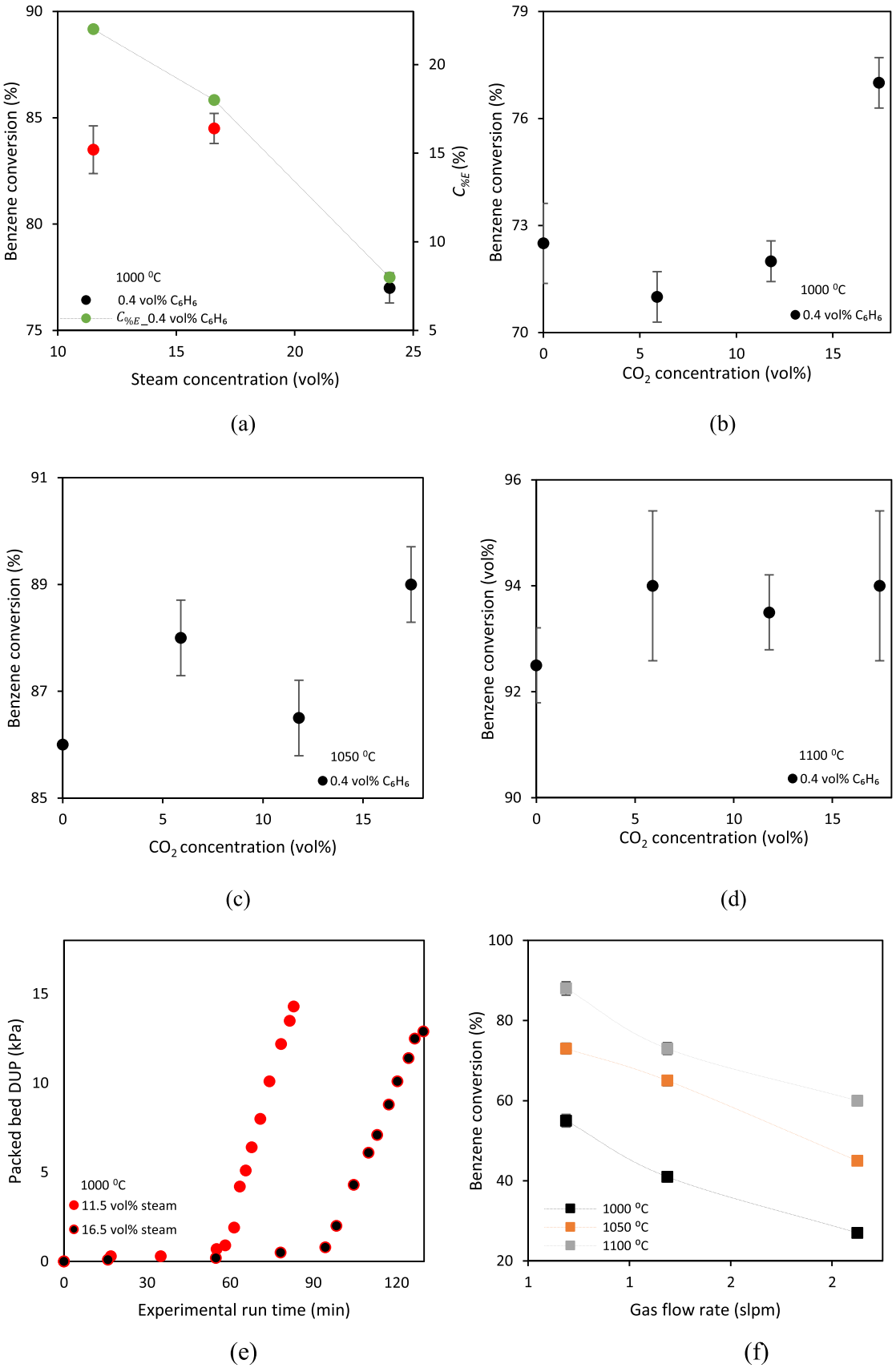

Fig. 6. Conversions of tested benzene concentrations at different steam concentrations in (a), CO_2 concentrations in (b-d) with red filled in symbols showing generation of coke, and corresponding rise in packed bed DUP during coke generation in (e) and benzene conversions at different gas flow rates and temperatures in (f).

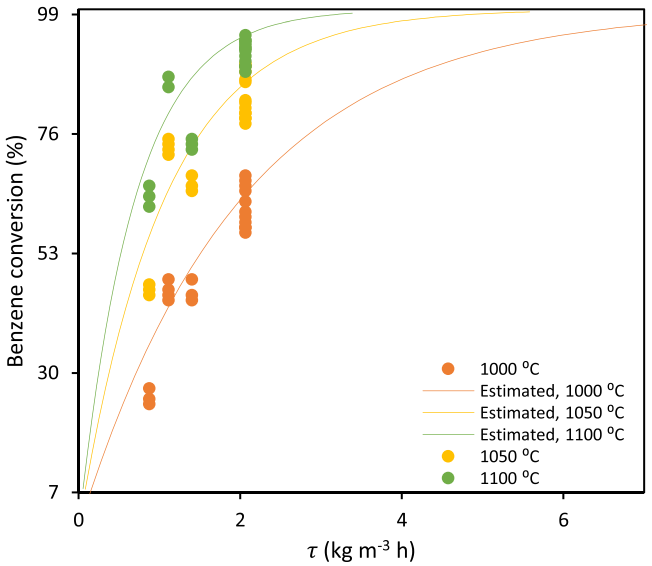

Fig. 7. Benzene conversions as a function of weight time (τ, kg m^{-3} h) at different temperatures as presented in Figs. 2–6.

Table 3
Estimated values of k for first order kinetic assumed benzene conversion at 1000–1100^0 ^{0}C.

Temperature (^{0}C)	1000	1050	1100
k (m^3 kg^{-1} h^{-1})	0.5	0.95	1.45

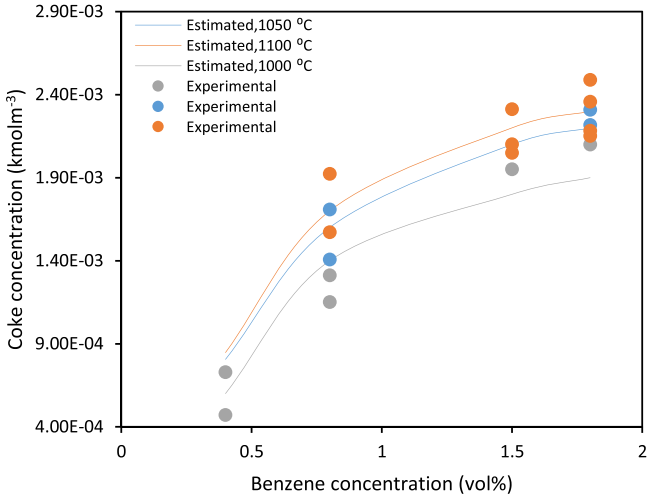

Fig. 8. Comparison of model estimated and experimentally determined coke.

Fig. 10 shows ln(k') of coke generated at different temperatures. Slightly higher k' for coke generated at 1000 ^{0}C than for coke generated at 1050 and 1100 ^{0}C are apparent. Computed E for oxidation of generated coke given in Table 4 show similar behavior; increasing E at increased temperature of coke generation.

6.2. FTIR

Fig. 11 shows the FTIR spectra of coke generated during benzene conversion at different temperatures. The spectra show just four absorption bands, which appear in between 400 and 1600 cm^{-1} and are due to well-defined chemical bonds. The absorption bands at 750, 760 and 880 cm^{-1} are interpreted as aromatic CH deformation (Vu et al., 2011). The fourth band at 1630 cm^{-1} represents the stretching vibrations of C═C in aromatic rings (Li et al., 2011). A decrease in intensities of absorption bands at increasing temperatures generated coke is apparent. Similar findings of significant influence of temperature on coke formation and structure have been reported (Zhang et al., 2014; Guisnet and Magnoux, 2001).

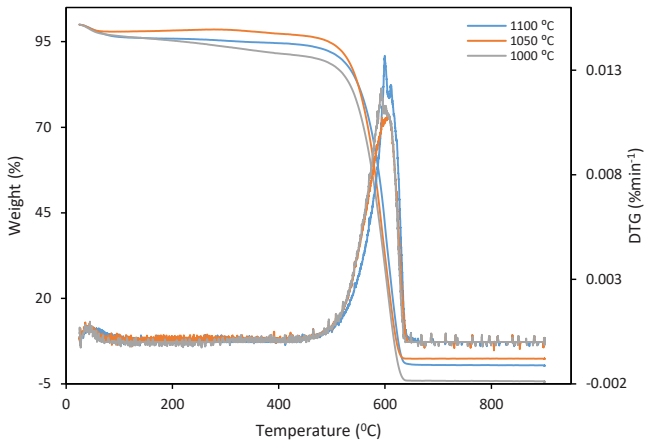

Fig. 9. TG/DTG curves for non-isothermal oxidation of coke generated during benzene conversion at different temperatures.

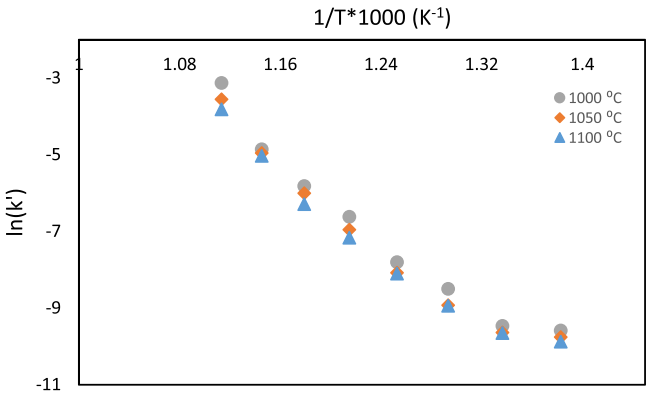

Fig. 10. Estimated logarithms of oxidation rate constants for non-isothermal oxidation of coke generated during benzene conversion at different temperatures.

Table 4
Activation energy and Arrhenius constant for non-isothermal oxidation of cokes generated at different temperatures.

Coke generation temperature (^{0}C)	E (kJmol^{-1})	A (10^9 min^{-1})
1000	189	1.16
1050	195	3.05
1100	197	5.62

7. Conclusion

In this study, different configurations of highly non-porous ɣ-Al_2O_3 packed bed reactor are tested to investigate any coke generation during conversion of tar model benzene at 1000–1100 ^{0}C. Considered configurations are mainly the modified packed beds with their different positions (relative to top (P_1), center (P_2) and bottom (P_3) of furnace), heights (5, 13 and 25 cm) and particles size (0.5, 3 and 5 mm). Experiments were performed using steam and CO_2 as reforming media for tested benzene concentrations (0.4–1.8 vol%). The results showed benzene conversions of 48–91% using a packed bed (height: 25 cm,

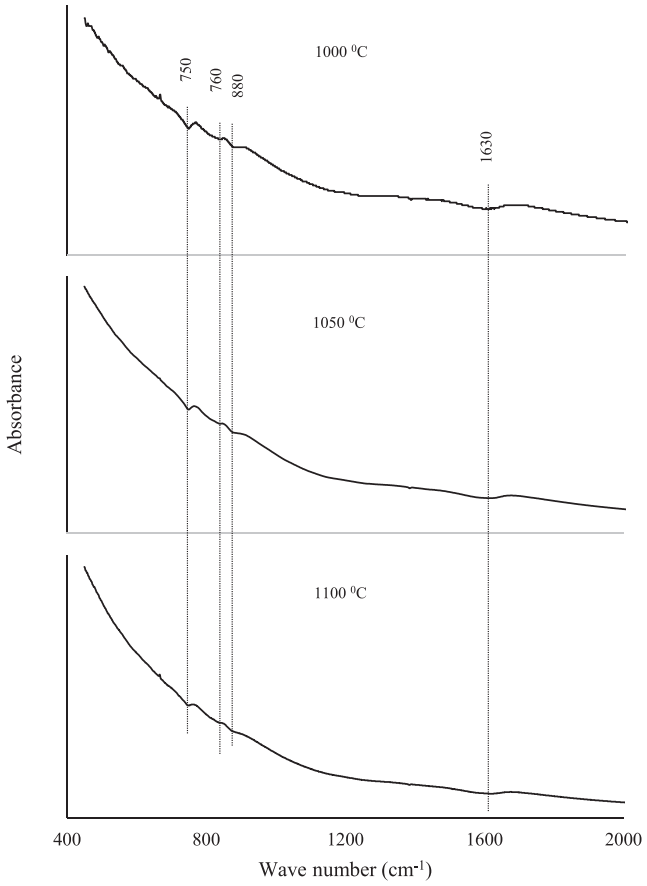

Fig. 11. FTIR spectra of coke generated during benzene conversion at different temperatures.

particles size: 3 mm) at P_1 with generation and deposition of steady thin coke on bed particles. Whereas relative high benzene conversions of 63–93 and 68–95% at P_2 and P_3 respectively at benzene concentrations greater than 0.4 vol% experienced continuous increases in differential upstream pressures (DUPs) of beds due to generation and accumulation of unsteady thick coke. Tested packed bed heights and particles sizes achieved similar benzene conversions at similar experimental conditions. Whereas, conversion of benzene concentrations greater than 0.8 vol% with packed bed heights of 5 and 13 cm and particles size of 0.5 mm at 1100 ^{0}C lead similar unsteady coke generation. Increased benzene polymerization and reduced bed surface gasification reactions due to improperly placed packed beds could be the main contributors towards generation of unsteady coke as obvious from its condensed structure evidenced through characterization. The developed kinetic model simulated well the observed coke generation. As conclusion, installation of a proper alumina packed bed based on tar concentration and other conditions could lead tar conversion without unsteady coke generation by limiting and facilitating the polymerization and gasification reactions respectively.

Declaration of Competing Interest

The authors declare that they have no known competing financial interests or personal relationships that could have appeared to influence the work reported in this paper.

Acknowledgements

The financial support provided via the Swedish Energy Agency and the Swedish Gasification Centre is gratefully acknowledged.

References

Ahmad, W., Lin, L., Strand, M., 2022. Benzene conversion using a partial combustion approach in a packed bed reactor. Energy 239, 122251.
Ahmad, W., Lin, L., Strand, M., 2023. Coke-free conversion of benzene at high temperatures. J. Energy Inst. 109, 101307.
Alexander, John D., W.L. Martin, John N. Dew, Factors affecting fuel availability and composition during in situ combustion. 1962. 14(10), 1154–1164.
Ashok, J., et al., 2020. Recent progress in the development of catalysts for steam reforming of biomass tar model reaction. Fuel Process. Technol. 199, 106252.
Brandt, P. , U.B. Henriksen. Decomposition of tar in pyrolysis gas by partial oxidation and thermal cracking: part 2. In: Proceedings of the Tenth European Conference and Technology Exhibition, 1998, Carmen.
Cao, J.-P., et al., 2018. Effect of atmosphere on carbon deposition of Ni/Al2O3 and Ni-loaded on lignite char during reforming of toluene as a biomass tar model compound. Fuel 217, 515–521.
de Caprariis, B., et al., 2019. Biomass gasification: the effect of the surface area of different materials on tar abatement efficiency, 34 (2), 1137–1144.
Chen, X., Ma, X., Peng, X., 2022. Role of reforming agent in filamentous coke deposition on Ni/bio-char catalyst during non-oxygenates tar reforming. Appl. Catal. A Gen. 630, 118446.
Cheng, L., et al., 2020. Tar elimination from biomass gasification syngas with bauxite residue derived catalysts and gasification char. Appl. Energy 258, 114088.
Dayton, D., Review of the Literature on Catalytic Biomass Tar Destruction: Milestone Completion Report. 2002.
Delgado, J., Aznar, M.P., Corella, J., 1996. Calcined dolomite, magnesite, and calcite for cleaning hot gas from a fluidized bed biomass gasifier with steam: life and usefulness. Ind. Eng. Chem. Res. 35 (10), 3637–3643.
Gao, R., et al., 2022. Development and application of Ni–M/sepiolite (M=Ce, Pr, and La) catalysts in biomass pyrolysis for syngas production. Energy Rep. 8, 5957–5964.
Gilbert, P., et al., 2009. Tar reduction in pyrolysis vapours from biomass over a hot char bed. Bioresour. Technol. 100 (23), 6045–6051.
Gómez-Barea, A., Leckner, B., 2010. Gasification of biomass and waste. In: Handbook of Combustion. Wiley, pp. 365–397.
Gómez Cápiro, O., et al., 2021. Carbothermic reduction of carbon aerogel-supported Fe during the catalytic decomposition of toluene. Catal. Today 372, 82–88.
Guisnet, M., Magnoux, P., 2001. Organic chemistry of coke formation. Appl. Catal. A Gen. 212 (1), 83–96.
Han, J., Kim, H., 2008. The reduction and control technology of tar during biomass gasification/pyrolysis: an overview. Renew. Sustain. Energy Rev. 12 (2), 397–416.

Hosokai, S., et al., 2005. Spontaneous generation of tar decomposition promoter in a biomass steam reformer. Chem. Eng. Res. Des. 83 (9), 1093–1102.
Hosokai, S., et al., 2008. Mechanism of decomposition of aromatics over charcoal and necessary condition for maintaining its activity, 87 (13–14), 2914–2922.
Houben, M., et al., 2002. An analysis and experimental investigation of the cracking and polymerisation of tar. In: Proceedings of the Twelfth European Biomass Conference.
Jess, A., 1996. Mechanisms and kinetics of thermal reactions of aromatic hydrocarbons from pyrolysis of solid fuels. Fuel 75 (12), 1441–1448.
Jess, A.J.E., Erdgas, Kohle, 1995. Reaktionskinetische untersuchungen zur thermischen zersetzung von modellkohlenwasserstoffen, 111(11), 479–484.
Kök, M.V., 2008. Non-isothermal kinetic analysis and feasibilty study of medium grade crude oil field. J. Therm. Anal. Calorim. 91 (3), 745–748.
Korus, A., et al., 2017. Pyrolytic toluene conversion to benzene and coke over activated carbon in a fixed-bed reactor. Fuel 207, 283–292.
Larsson, A., et al., 2021. Steam gasification of biomass – typical gas quality and operational strategies derived from industrial-scale plants. Fuel Process. Technol. 212, 106609.
Li, J., et al., 2021a. Investigation of coke deposition during catalytic cracking of different biomass model tar: effect of microwave. Appl. Catal. A Gen. 624, 118325.
Li, J., et al., 2022. Synergistic effect of hydrogen atmosphere and biochar catalyst on tar decomposition and methane-rich gas production during biomass pyrolysis. Fuel 330, 125680.
Li, Q., et al., 2011. Coke formation on Pt–Sn/Al2O3 catalyst in propane dehydrogenation: coke characterization and kinetic study. Top. Catal. 54 (13), 888.
Li, X., et al., 2021b. Effect of volatiles' reaction on coking of tar during pyrolysis of Naomaohu coal in a downer-bed reactor. Fuel Process. Technol. 212, 106623.
Lin, L., Strand, M., 2013. Investigation of the intrinsic CO_2 gasification kinetics of biomass char at medium to high temperatures. Appl. Energy 109, 220–228.
Lin, L., Strand, M., 2014. Online investigation of steam gasification kinetics of biomass chars up to high temperatures. Energy Fuels 28 (1), 607–613.
Liu, T.-L., et al., 2017. In situ upgrading of Shengli lignite pyrolysis vapors over metal-loaded HZSM-5 catalyst. Fuel Process. Technol. 160, 19–26.
Madadkhani, S., et al., 2021a. Bauxite residue as an iron-based catalyst for catalytic cracking of naphthalene, a model compound for gasification tar. Can. J. Chem. Eng. 99 (7), 1461–1474.
Madadkhani, S., et al., 2021b. Bauxite residue as an iron-based catalyst for catalytic cracking of naphthalene, a model compound for gasification tar, 99 (7), 1461–1474.
Morgalla, M., Lin, L., Strand, M., 2018a. Benzene conversion in a packed alumina bed continuously fed with woody char particles. Energy Fuels 32 (7), 7670–7677.
Morgalla, M., Lin, L., Strand, M., 2018b. Benzene conversion in a packed bed loaded with biomass char particles. Energy Fuels 32 (1), 554–560.
Narváez, I., Corella, J., Orío, A., 1997. Fresh tar (from a Biomass Gasifier) elimination over a commercial steam-reforming catalyst. Kinet. Eff. Differ. Var. Oper. Ind. Eng. Chem. Res. 36 (2), 317–327.
Ranjbar, M., 1995. Improvement of medium and light oil recovery with thermocatalytic in situ combustion. J. Can. Pet. Technol. 34 (08).
Ren, Y., Mahinpey, N., Freitag, N., 2007. Kinetic model for the combustion of coke derived at different coking temperatures. Energy Fuels 21 (1), 82–87.
Serio, M.A., et al., Kinetics of Vapor-phase Secondary Reactions of Prompt Coal Pyrolysis Tars, 1987, 26(9), 1831–1838.
Shen, Y., Fu, Y., 2018. Advances in in situ and ex situ tar reforming with biochar catalysts for clean energy production. Sustain. Energy Fuels 2 (2), 326–344.
Shen, Y., Yoshikawa, K., 2013. Recent progresses in catalytic tar elimination during biomass gasification or pyrolysis—a review. Renew. Sustain. Energy Rev. 21, 371–392.
Shen, Y., Yoshikawa, K.J.R., Reviews, S.E., 2013. Recent progresses in catalytic tar elimination during biomass gasification or pyrolysis—a review, 21, 371–392.
Shimizu, T., et al., 2007. Capacitance effect of porous solids: an approach to improve fluidized bed conversion processes of high-volatile fuels. Chem. Eng. Sci. 62 (18), 5549–5553.
Sun, H., et al., 2021a. Effect of steam on coke deposition during the tar reforming from corn straw pyrolysis over biochar. Fuel Process. Technol. 224, 107007.
Sun, H., et al., 2021b. Mechanism of coke formation and corresponding gas fraction characteristics in biochar-catalyzed tar reforming during corn straw pyrolysis. Fuel Process. Technol. 221, 106903.
Sun, H., et al., 2022. Roles of AAEMs in catalytic reforming of biomass pyrolysis tar and coke accumulation characteristics over biochar surface for H2 production. Int. J. Hydrog. Energy 47 (68), 29207–29218.
Tian, Y., et al., 2022a. The study of coke resistance of Ni/ZrO2 by core-shell structure coupling with cobalt doping modification in CO_2 reforming of tar. Appl. Catal. A Gen. 643, 118797.
Tian, Y., et al., 2022b. The influence of shell thickness on coke resistance of core-shell catalyst in CO_2 catalytic reforming of biomass tar. Int. J. Hydrog. Energy 47 (29), 13838–13849.
Virk, P.S., Chambers, L.E., Woebcke, H.N., 1974. Thermal hydrogasification of aromatic compounds. In: Coal Gasification. American Chemical Society, pp. 237–258.
Vu, B.K., et al., 2011. Electronic density enrichment of Pt catalysts by coke in the propane dehydrogenation. Korean J. Chem. Eng. 28 (2), 383–387.
Wang, J., et al., 2022. Catalytic activity evaluation and deactivation progress of red mud/carbonaceous catalyst for efficient biomass gasification tar cracking, 323, 124278.
Wang, L., et al., 2011. Catalytic performance and characterization of Ni-Fe catalysts for the steam reforming of tar from biomass pyrolysis to synthesis gas. Appl. Catal. A Gen. 392 (1), 248–255.
Wang, S., et al., 2020. Pyrolysis municipal sludge char supported Fe/Ni catalysts for catalytic reforming of tar model compound. Fuel 279, 118494.
Watanabe, H., et al., Development on Numerical Simulation Technology of Heavy Oil Gasifier. 2002. 1023, 2002.
Wu, J., et al., 2017. Coke formation during thermal reaction of tar from pyrolysis of a subbituminous coal. Fuel Process. Technol. 155, 68–73.
Wu, W.-g, et al., 2011. Experimental investigation of tar conversion under inert and partial oxidation conditions in a continuous reactor. Energy Fuels 25 (6), 2721–2729.
Xu, W.-C., Tomita, A., 1989. The effects of temperature and residence time on the secondary reactions of volatiles from coal pyrolysis. Fuel Process. Technol. 21 (1), 25–37.
Zeng, X., et al., 2018. Characteristics of tar abatement by thermal cracking and char catalytic reforming in a fluidized bed two-stage reactor. Fuel 231, 18–25.
Zhai, M., et al., 2015. Characteristics of rice husk tar secondary thermal cracking. Energy 93, 1321–1327.
Zhang, H., et al., 2014. Characterization of coke deposition in the catalytic fast pyrolysis of biomass derivates. Energy Fuels 28 (1), 52–57.
Zhang, S., et al., 2021. Catalytic cracking of biomass tar using Ni nanoparticles embedded carbon nanofiber/porous carbon catalysts. Energy 216, 119285.
Zhang, S., et al., 2023. Investigation into biochar supported Fe-Mo carbides catalysts for efficient biomass gasification tar cracking. Chem. Eng. J. 454, 140072.
Zhang, Y., et al., 2006. Peculiarities of rapid pyrolysis of biomass covering medium- and high-temperature ranges. Energy Fuels 20 (6), 2705–2712.
Zhang, Y., et al., 2010. Tar destruction and coke formation during rapid pyrolysis and gasification of biomass in a drop-tube furnace. Fuel 89 (2), 302–309.